Electronic Supplementary Information

Largely Boost Methanol Electrooxidation Using Ionic Liquid/PdCu Aerogels via Interface Engineering

Hengjia Wang,[a] Songlin Zhang,[b] Weiwei Cai,[c] Bo Z. Xu,[d] Zhixiang Cai,[b] Yu Wu,[a] Xin Luo,[a] Xiaoqian Wei,[a] Zhao Liu,[c] Wenling Gu,[a] Alexander Eychmüller,[e] Chengzhou Zhu*[a] and Jun Chen*[b]

[a]Key Laboratory of Pesticide and Chemical Biology of Ministry of Education, International Joint Research Center for Intelligent Biosensing Technology and Health, College of Chemistry, Central China Normal University, Wuhan 430079, People's Republic of China.

[b]Department of Bioengineering, University of California, Los Angeles, Los Angeles, CA 90095, United States.

[c]Sustainable Energy Laboratory, Faculty of Materials Science and Chemistry, China University of Geosciences, Wuhan 430074, People's Republic of China.

[d]School of Mechanical and Materials Engineering, Washington State University, Pullman, WA 99164, United States.

[e]Physikalische Chemie, Technische Universität Dresden, Bergstraße 66b, 01062 Dresden, Germany.

*Corresponding Authors: czzhu@mail.ccnu.edu.cn (C. Z.); jun.chen@ucla.edu (J. C.)

Experimental Section

Chemicals

Sodium borohydride ($NaBH_4$, 98%, powder) and Nafion solution (5 wt %) were purchased from Sinopharm Chemical Reagent Co. Let (Shanghai, China). Palladium (II) chloride and copper chloride were purchased from Aladdin Industrial Corporation. Palladium on activated carbon powder (20% Pd loading, nominally 50% water wet) was purchased from Alfa Aesar. H_2PdCl_4 was prepared by dissolving $PdCl_2$ in the HCl solution. KOH was obtained from China National Medicines Corporation Ltd. Unless otherwise stated, other reagents were of analytical grade and were used as received. The water in all experiments was prepared in a three-stage Millipore Milli-Q plus 185 purification system and had a resistivity higher than 18.2 MΩ cm.

Apparatus

X-ray Diffraction (XRD) characterization was carried out by a D8 ADVANCE (Bruker, Germany). Scanning electron microscope (SEM) image was obtained by a Quanta FEG250 field-emission environmental SEM (FEI, United States). Transmission electron microscope (TEM) images were from a Titan G260-300 (Thermo Fisher, United States). X-ray photoelectron spectroscopy (XPS) measurements were performed by a VG Multilab 2000 (Thermo Fisher, United States). Supercritical CO_2 drying was conducted using an SPI-Dry™ critical point drying apparatus (SPI Supplies, USA). The content of each element in the samples was determined by inductively coupled plasma optical emission spectrometry (ICP-OES) (Agilent 8800). The contact angle was

measured on a Model 200 video-based optical contact angle measuring instrument (Future Scientific Ltd. Co., Taiwan, China).

Synthesis of IL/PdCu hydrogels/aerogels

1-(3-aminopropyl)-3-methylimidazolium bromide (IL–NH_2) was first prepared according to a previously reported method.[1] In the typical synthesis of IL/Pd_3Cu_1 metallic hydrogel, aqueous $NaBH_4$ (2 mL, 0.05 M) was quickly injected into 35 mL of aqueous solution that contained H_2PdCl_4 (0.375 mM), $CuCl_2$ (0.125 mM) and 0.25 Mm IL-NH_2 under stirring at 60 °C for 1 min. The resulting solution was allowed to settle still at 60 °C. After about 1 hour, IL/Pd_3Cu_1 hydrogel was generated at the bottom of the vial. After carefully washing with water for three times and replacing the supernatant by acetone, IL/Pd_3Cu_1 aerogel could be obtained from supercritical drying. Furthermore, all IL/Pd_xCu (x=1,5) hydrogels were obtained via the same method only except changing the mole ratio of Pd and Cu precursors. Pd_3Cu_1 metallic hydrogel was also obtained with the same method except without the addition of IL-NH_2.

Electrochemical measurements

All electrochemical measurements were processed with a standard three-electrode system by using an electrochemical workstation (CHI-660) at room temperature. The catalyst-modified glassy carbon electrode (GCE, 3 mm diameter) acts as the working electrode, a Hg/$HgCl_2$ electrode filled with saturated potassium chloride aqueous solution as the reference electrode and a Pt wire as the counter electrode. The GCE was prepared by polishing with 1.0 and 0.05 μm alumina powder, respectively, and rinsed with deionized water. For the methanol oxidation reaction, 5 μL of the as-obtained

aerogels (0.2 mg_{Pd}/mL) or Pd/C catalyst (0.2 mg_{pd} /mL) aqueous solution was dropped on the surface of the GCE and dried at 50 °C, followed by dropping 3 μL of Nafion (0.05 %) and dried at 50 °C.

Membrane electrode assembly (MEA) preparation and the DMFCs tests

The catalyst ink was prepared using the following weight ratio: catalyst/isopropanol/deionized water/5 wt% Nafion of 1/12/12/11. The catalyst ink was sprayed onto one side of a 5 cm^2 carbon paper (TGP-H-060, Toray) after ultrasonic treatment for 1 h until the loading reached 2 mg cm^{-2}. The prepared catalysts (or commercial Pd black) were used as anode catalyst while 20 wt.% Pt/C was used as a cathode catalyst. The anode electrode, porous membrane and cathode electrode were then assembled with the fuel reservoir and current collectors by screws at a certain pressure to form a passive fuel cell. 5 M KOH + 1 M methanol solution was used as fuel and electrolyte and ambient air was used as the oxidant. Polarization curves of the air-breathing fuel cells were collected by an Arbin battery test system at 25 °C.

First-Principles Calculations

To study the different performance, first-principles, density functional theory (DFT) calculations were performed using the method encoded in the Quantum ESPRESSO software package.[2,3] The local density approximation (LDA) functional was used for the exchange-correlation energy and norm-conserving Trouiller-Martins type pseudopotentials were used in place of all electron atomic potentials.[4,5] The wave function was expressed as a plane-wave summation truncated at an energy cutoff of 1020 eV and Kohn-Sham energies were sampled across the Brillouin zone using a

4×4×1 Monkhorst-Pack grid[6] to ensure that the calculated forces were converged to better than 5 meV/Å. The CO adsorption on the above structures was calculated. The CO adsorption process can be summarized as follow:

$$* + CO \rightarrow * CO$$

Where * represents active sites. The Gibbs free energy change associated with this process is calculated by:

$E = E_{sur+CO} - E_{CO} - E_{sur}$

Where E_{sur} is the total energy of the reactant surfaces, E_{sur+CO} is the total energy of product surfaces.

Supplementary Figures

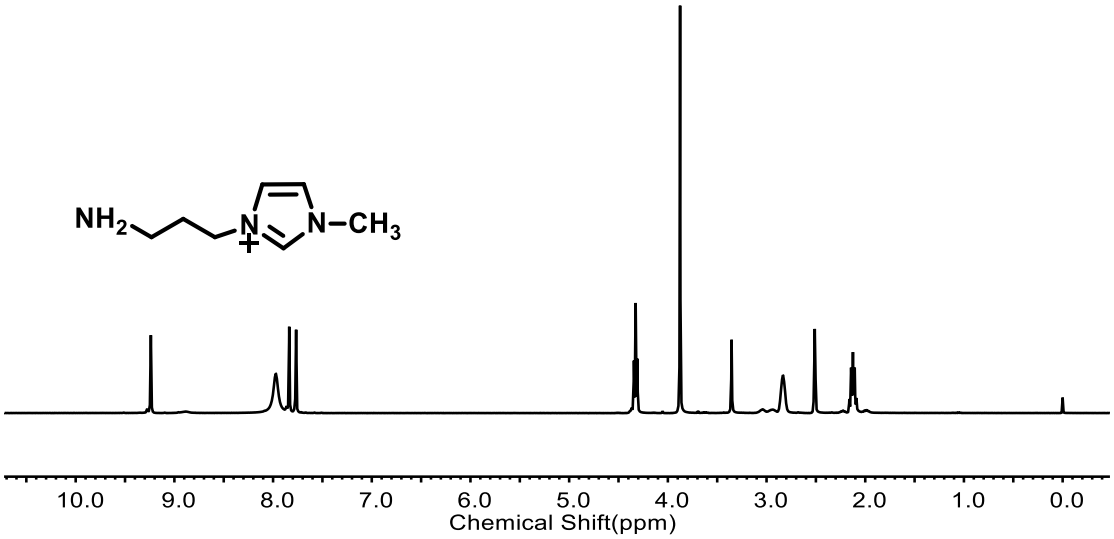

Figure S1. ^{1}H NMR spectrum of 1-(3-aminopropyl)-3-methylimidazolium bromide (400 MHz, d_6-DMSO).

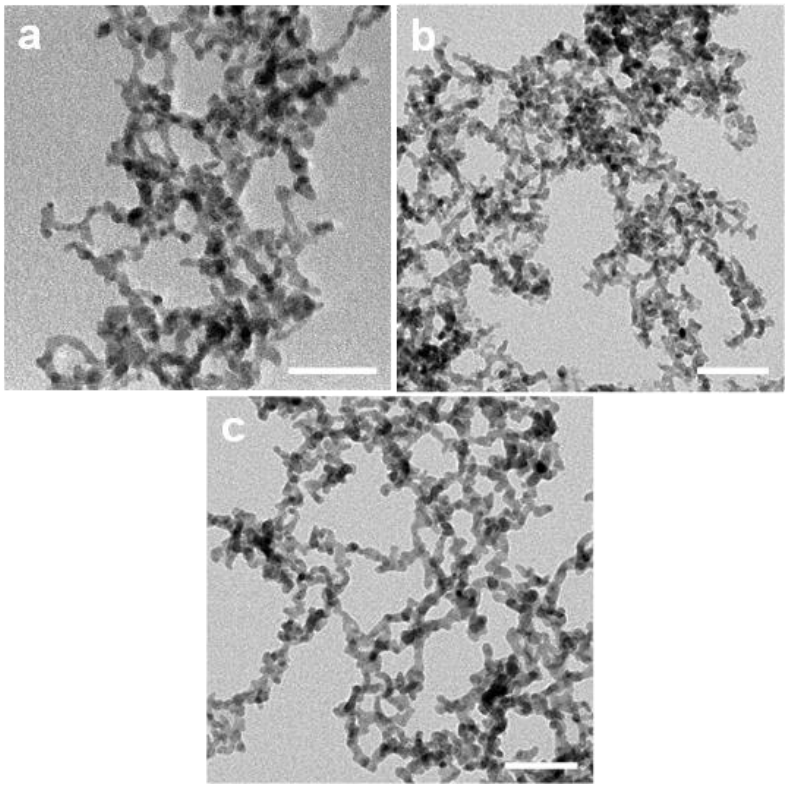

Figure S2. TEM images of Pd_3Cu_1 (a), IL/Pd_1Cu_1 (b) and IL/Pd_5Cu_1 (c) aerogels (scale bars, 50 nm).

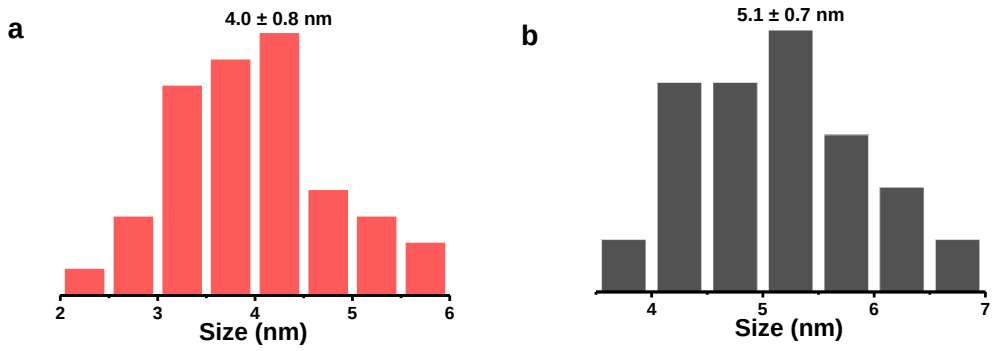

Figure S3. Size distributions of the backbone of IL/Pd_3Cu_1 (a) and Pd_3Cu_1 aerogels (b).

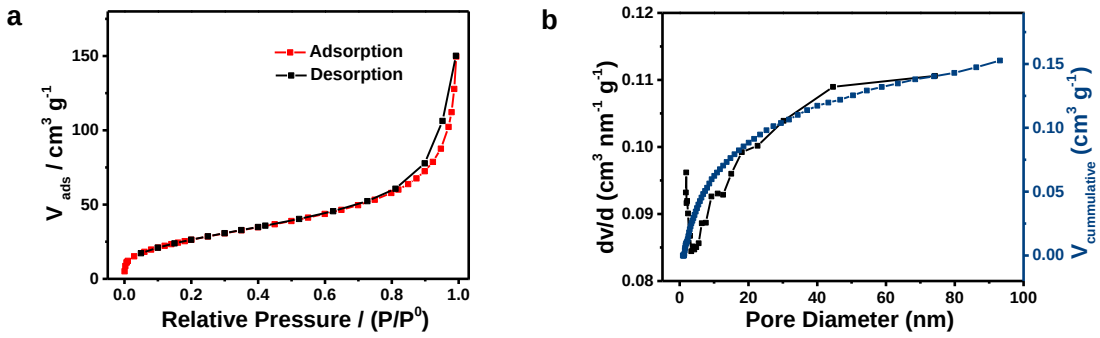

Figure S4. Nitrogen physisorption isotherm (a) and pore size distribution (b) of Pd_3Cu_1 aerogels.

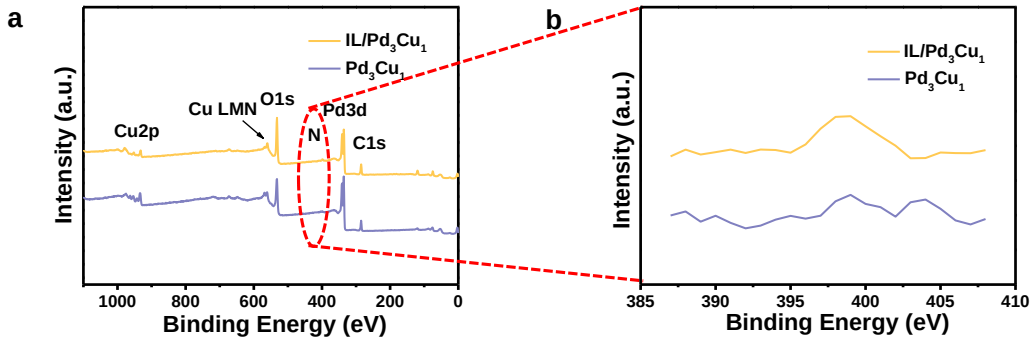

Figure S5. XPS spectra (a) and XPS patterns of IL/Pd_3Cu_1 and Pd_3Cu_1 aerogels (b).

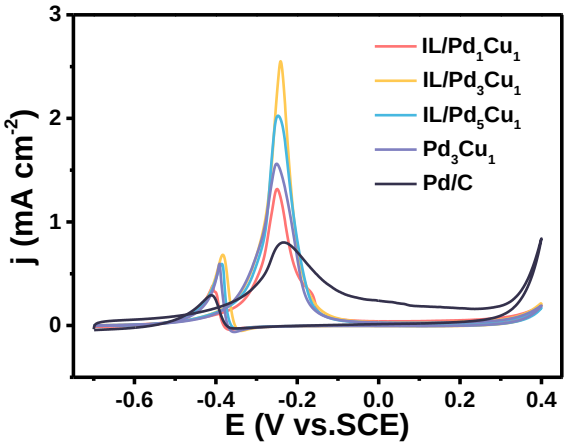

Figure S6. The ECSA-normalized CV curves of different electrocatalysts in 1.0 M KOH + 1.0 M methanol solution at a scan rate of 50 mV s^{-1}.

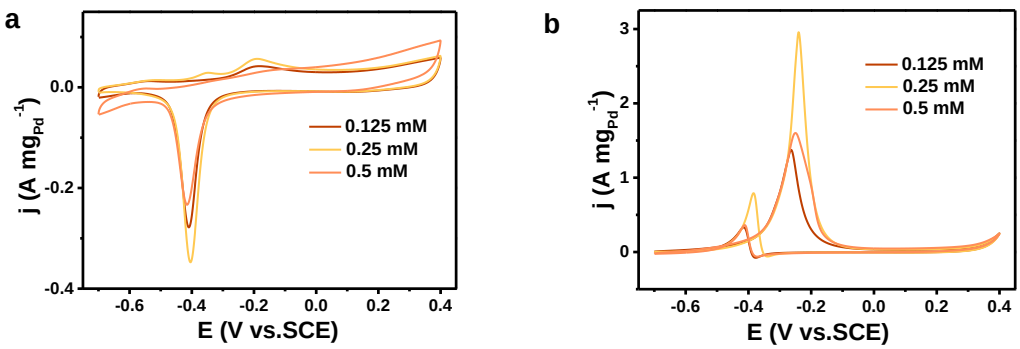

Figure S7. The influence of IL concentration on MOR. CV curves of Pd_3Cu_1 aerogels with different concentrations of IL in nitrogen-saturated 1.0 M KOH aqueous solution without (a) and with (b) 1 M methanol.

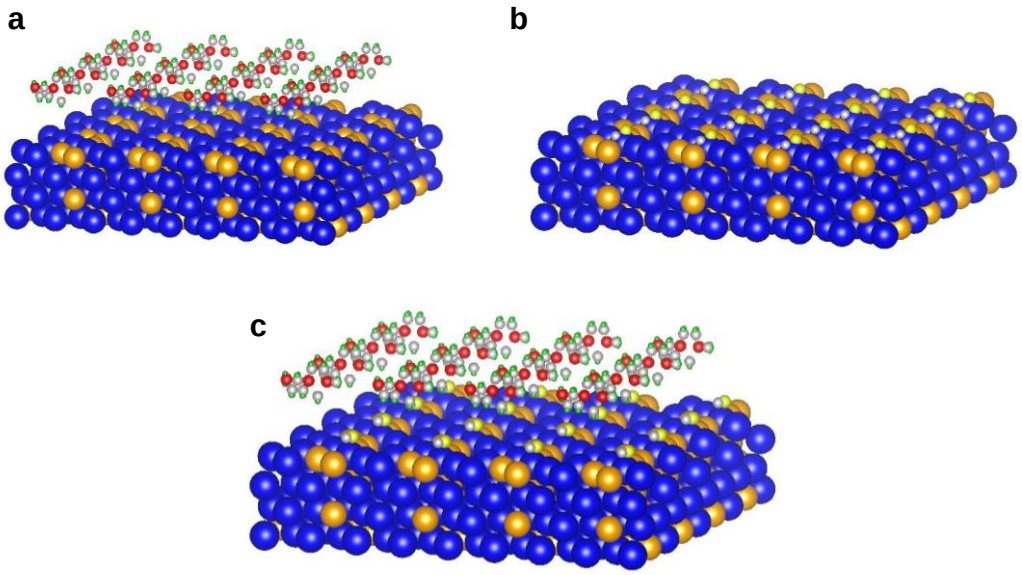

Figure S8. Theoretical simulation structure on the adsorption behavior of CO molecule. (a) The structural models of IL/Pd_3Cu_1 aerogels. The structures of CO adsorption on Pd_3Cu_1 (b) and IL/Pd_3Cu_1 (c) in the DFT calculations.

Supplementary Tables

Table S1. The composition of the IL/Pd_1Cu_1, IL/Pd_3Cu_1, Pd_3Cu_1 and IL/Pd_5Cu_1 aerogels by ICP-OES.

Samples	Pd (%)	Cu (%)
IL/Pd_1Cu_1	48.81	51.19
IL/Pd_3Cu_1	74.38	25.62
Pd_3Cu_1	71.62	28.38
IL/Pd_5Cu_1	83.65	16.35

Table S2. Comparison of the ECSA values, forward current density, backward current density and the ratio of the I_f and I_b of PdCu aerogels with different compositions and commercial Pd/C catalysts.

Samples	ECSA ($m^2\ g^{-1}$)	I_f ($A\ mg_{Pd}^{-1}$)	I_b ($A\ mg_{Pd}^{-1}$)	I_f/I_b
IL/Pd_1Cu_1	114.8	1.57	0.44	3.43
IL/Pd_3Cu_1	115.9	2.96	0.79	3.75
IL/Pd_5Cu_1	111.3	2.26	0.66	3.42
Pd_3Cu_1	111.2	1.74	0.66	2.64
Commercial Pd/C	43.9	0.35	0.13	2.69

Table S3. The mass activity of Pd-based nanomaterials for MOR in alkaline solution for nearly 6 years.

Catalysts	Electrolyte	Mass activity	References
IL/Pd_3Cu_1 aerogels	**1.0 M KOH+1.0 M CH_3OH**	**2.96 A mg_{Pd}^{-1}**	**This work**
Pd/ZC-1000	1.0 M KOH+1.0 M CH_3OH	0.873 A mg^{-1}	2015[7]
$Pd_{83}Ni_{17}$ Nanostructures	1.0 M KOH+1.0 M CH_3OH	1.11 A mg_{Pd}^{-1}	2015[8]
Pd/NS-G	0.5 M NaOH+1.0 M CH_3OH	0.399 A mg_{Pd}^{-1}	2016[9]
Pd_2P_1 porous network	1.0 M KOH+1.0 M CH_3OH	0.844 A mg_{Pd}^{-1}	2016[10]
PdCu-5 nanocages	1.0 M KOH+1.0 M CH_3OH	1.09 A mg_{Pd}^{-1}	2018[11]
Pd–Ni MCs-2	0.5 M KOH+1.0 M CH_3OH	0.525 A mg_{Pd}^{-1}	2018[12]
Pd_3Pb NSAs/C	**1.0 M KOH+1.0 M CH_3OH**	**2.98 A mg_{Pd}^{-1}**	**2018[13]**
PdCo J-NWs	1.0 M KOH+1.0 M CH_3OH	1.205 A mg_{Pd}^{-1}	2018[14]
20% Pd/SA	1.0 M KOH+1.0 M CH_3OH	0.336 A mg_{Pd}^{-1}	2018[15]
Pd/MGF	1.0 M KOH+1.0 M CH_3OH	0.835 A mg_{Pd}^{-1}	2019[16]
β-PdH cubes/C	0.5 M KOH+1.0 M CH_3OH	1.56 A mg_{Pd}^{-1}	2019[17]
PdCuRu NSs	1.0 M KOH+1.0 M CH_3OH	1.66 A mg_{Pd}^{-1}	2019[18]
Ni-Supported Pd Nanoparticles	1.0 M NaOH+0.5 M CH_3OH	1.02 A mg_{Pd}^{-1}	2019[19]
Pd(20%)-CeO_2(20%)/NMCS	1.0 M KOH+1.0 M CH_3OH	1.5 A mg^{-1}	2019[20]
$Pd_{0.52}Ag$/CNTs	0.5 M NaOH+1.0 M CH_3OH	0.72 A mg_{Pd}^{-1}	2019[21]
Pd Nanowire@cCuO_x	1.0 M KOH+1.0 M CH_3OH	0.54 A mg_{Pd}^{-1}	2019[22]
PdO/Pd	1.0 M KOH+1.0 M CH_3OH	1.111 A mg^{-1}	2020[23]
Pd-NiO-Y/CNT	**1.0 M NaOH+1.0 M CH_3OH**	**3.9 A mg_{Pd}^{-1}**	**2020[24]**

Table S4. The composition of the Pd_3Cu_1 and IL/Pd_3Cu_1 aerogels before and after the chronoamperometric experiments by ICP-OES.

Samples	Pd (%)	Cu (%)
IL/Pd_3Cu_1	74.38	25.62
	89.18	10.82
Pd_3Cu_1	71.62	28.38
	90.88	9.12

Table S5. The different IL concentrations of Pd_3Cu_1 aerogels by ICP-OES.

Samples	Pd (%)	Cu (%)
IL (0.125 mM)	74.25	25.75
IL (0.5 mM)	74.57	25.43

Supplementary References

1. C. Zhu, J. Zhai and S. Dong, *Nanoscale*, 2014, **6**, 10077-10083.
2. W. Kohn and L. J. Sham, *Phys. Rev.*, 1965, **140**, 1133-1138.
3. P. Giannozzi, S. Baroni, N. Bonini, M. Calandra, R. Car, C. Cavazzoni, D. Ceresoli, G. L Chiarotti, M. Cococcioni, I. Dabo, A. Dal Corso, S. de Gironcoli, S. Fabris, G. Fratesi, R. Gebauer, U. Gerstmann, C. Gougoussis, A. Kokalj, M. Lazzeri, L. Martin-Samos, N. Marzari, F. Mauri, R. Mazzarello, S. Paolini, A. Pasquarello, L. Paulatto, C. Sbraccia, S. Scandolo, G. Sclauzero, A. P. Seitsonen, A. Smogunov, P. Umari and R. M. Wentzcovitch, *J. Phys. Condens. Matter*, 2009, **21**, 395502.
4. J. P. Perdew and Y. Wang, *Phys. Rev. B*, 1992, **45**, 13244-13249.
5. N. Troullier and J. L. Martins, *Phys. Rev. B*, 1991, **43**, 1991-1997.
6. H. Monkhorst and J. Pack, *Phys. Rev. B*, 1976, **13**, 5188-5192.
7. J. Li, Q. Zhu and Q. Xu, *Chem. Commun.*, 2015, **51**, 10827-10830.
8. C. Zhu, D. Wen, M. Oschatz, M. Holzschuh, W. Liu, A. K. Herrmann, F. Simon, S. Kaskel and A. Eychmüller, *Small*, 2015, **11**, 1430-1434.
9. X. Zhang, J. Zhu, Zhang, X.; C. Tiwary, Z. Ma, H. Huang, J. Zhang, Z. Lu, W. Huang ang Y. Wu, *ACS Appl. Mater. Interfaces*, 2016, **8**, 10858-10865.
10. K. Zhang, C. Wang, D. Bin, J. Wang, B. Yan, Y. Shiraishi, Y. Du, *Catal. Sci. Technol.*, 2016, **6**, 6441-6447.
11. J. Sheng, J. Kang, H. Ye, J. Xie, B. Zhao, X.-Z. Fu, Y. Yu, R. Sun and C.-P. Wong, *J. Mater. Chem. A*, 2018, **6**, 3906-3912.
12. M. Zhao, Z. Kang, Q. Chen, X. Yu, Y. Wu, X. Fan, X. Yan, Y. Lin, T. Xia and W. Cai, *J. Mater. Chem. A*, 2018, **7**, 5179-5184.
13. L. Bu, C. Tang, Q. Shao, X. Zhu and X. Huang, *ACS Catal.*, 2018, **8**, 4569-4575.
14. J. Fan, S. Yu, K. Qi, C. Liu, L. Zhang, H. Zhang, X. Cui and W. Zheng, *J. Mater. Chem. A*, 2018, **6**, 8531-8536.
15. C. Wang, L. Zheng, R. Chang, L. Du, C. Zhu, D. Geng, D. Yang, *ACS Appl. Mater. Interfaces*, 2018, **10**, 29965-29971.
16. X. Cui, Y. Li, M. Zhao, Y. Xu, L. Chen, S. Yang and Y. Wang, *Nano Res.*, 2019, **12**, 351-356.

17. M. Kabiraz, J. Kim, W. Lee, B. Ruqia, H. Kim, S. Lee, J. Kim, S. Paek, J. Hong and S. Choi, *Chem. Mater.*, 2019, **31**, 5663-5673.
18. L. Jin, H. Xu, C. Chen, H. Shang, Y. Wang, C. Wang and Y. Du, *ACS Appl. Mater. Interfaces*, 2019, **11**, 42123-42130.
19. H. Lei, X. Li, C. Sun, J. Zeng, S. Siwal and Q. Zhang, *Small*, 2019, 1804722.
20. Q. Tan, C. Shu, J. Abbott, Q. Zhao, L. Liu, T. Qu, Y. Chen, H. Zhu, Y. Liu and G. Wu, *ACS Catal.*, 2019, **9**, 6362-6371.
21. L. Huang, J. Zou, J. Ye, Z. Zhou, Z, Lin, X. Kang, P. Jain and S. Chen, *Angew. Chem. Int. Ed.*, 2019, **58**, 8794 -8798.
22. Z. Chen, Y. Liu, C. Liu, J. Zhang, Y. Chen, W. Hu and Y. Deng, *Small*, 2019, 1904964.
23. T. Wang, F. Li, H. Huang, S. Yin, P. Chen, P. Jin and Y. Chen, *Adv. Funct. Mater.*, 2020, 2000534.
24. M. Sharma, B. Das, M. Baruah, P. Bhattacharyya, L. Saikia and K. Bania, *Chem. Commun.*, 2020, **56**, 375-378.